Neuro-Oncology Advances
4(1), 1–12, 2022 | https://doi.org/10.1093/noajnl/vdac028 | Advance Access date 28 February 2022

Filamin A increases aggressiveness of human neuroblastoma

Sashidar Bandaru, Bharat Prajapati, Prasanna Kumar Juvvuna, Sandor Dosa, Per Kogner, John I. Johnsen, Chandrasekhar Kanduri, and Levent M. Akyürek

Department of Clinical Pathology, Sahlgrenska University Hospital, Region Västra Götaland, Göteborg, Sweden (S.B., S.D., L.M.A.); Department of Laboratory Medicine, Institute of Biomedicine, University of Gothenburg, Göteborg, Sweden (S.B., L.M.A.); Department of Medical Biochemistry and Cell Biology, Institute of Biomedicine, University of Gothenburg, Göteborg, Sweden (B.P., P.K.J., C.K.); Childhood Cancer Research Unit, Department of Women´s and Children's Health, Karolinska Institute, Stockholm, Sweden (P.K, J.I.J.)

Corresponding Authors: Sashidar Bandaru, PhD, Department of Clinical Pathology, Region Västra Götaland, Sahlgrenska University Hospital, Göteborg, Sweden (sashidar.bandaru@medkem.gu.se); Levent M. Akyürek, MD, PhD, Department of Clinical Pathology, Region Västra Götaland, Sahlgrenska University Hospital, Göteborg, Sweden (levent.akyurek@vgregion.se).

Abstract

Background. The actin-binding protein filamin A (FLNA) regulates oncogenic signal transduction important for tumor growth, but the role of FLNA in the progression of neuroblastoma (NB) has not been explored.

Methods. We analyzed *FLNA* mRNA expression in the R2 NB-database and FLNA protein expression in human NB tumors. We then silenced *FLNA* expression in human SKNBE2 and IMR32 NB cells by lentiviral vector encoding shRNA *FLNA* and assayed the cells for proliferation, migration, colony, spheroid formation, and apoptosis. SKNBE2 xenografts expressing or lacking FLNA in BALB/c nude mice were analyzed by both routine histopathology and immunohistochemistry.

Results. We observed shorter patient survival with higher expression of *FLNA* mRNA than patients with lower *FLNA* mRNA expression, and high-risk NB tumors expressed higher FLNA levels. Overexpression of FLNA increased proliferation of SH-SY5 NB cells. NB cell lines transfected with siRNA *FLNA* proliferated and migrated less, expressed lower levels of phosphorylated AKT and ERK1/2, formed smaller colonies and spheroids, as well as increased apoptosis. After inoculation of SKNBE2 cells infected with lentivirus expressing shRNA *FLNA*, size of NB tumors and number of proliferating cells were decreased. Furthermore, we identified STAT3 as an interacting partner of FLNA. Silencing *FLNA* mRNA reduced levels of NF-κB, STAT3 and MYCN, and increased levels of p53 and cleaved caspase 3.

Conclusion. Inhibition of FLNA impaired NB cell signaling and function and reduced NB tumor size *in vivo*, suggesting that drugs targeting either FLNA or its interaction with STAT3 may be useful in the treatment of NB.

Key Points

- Increased expression of FLNA in neuroblastomas.
- FLNA mediates STAT3-MYCN axis in neuroblastomas.

Neuroblastoma (NB) is a tumor derived from primitive cells of the sympathetic nervous system and is the most common solid tumor in children.[1] Children with high-risk NB require more aggressive treatment, which often includes chemotherapy, surgery, radiation, stem cell transplant, immunotherapy, and retinoid therapy. NB is a primitive neoplasm of neuroectodermal origin and is composed of immature neuroblasts.[2] Histomorphologically, NB is further subcategorized regarding the amount of the differentiating neuroblasts and the amount of the neuropil created by the NB cells defined by the International Neuroblastoma Pathology Classification (INPC).[2] Rarely neuroblasts may display anaplastic, pleomorphic, spindled, or pseudorhabdoid features. According to the Children's

Importance of the Study

Our study shows that increased expression of FLNA associates with shorter survival rate and high-risk NB tumors. Silencing of FLNA leads to impaired proliferation, migration, and colony formation, as well as increased apoptosis of NB cells *in vitro* and NB cells lacking FLNA form smaller tumors *in vivo*. Furthermore, FLNA binds to STAT3, regulating of MYCN. Thus, our study identifies FLNA as a potential target to reduce NB growth.

Oncology Group the recent NB risk grouping system includes age, MYCN status, and INPC histology with notes on surgical resection.[3] Although clonal proliferation of immature cells of neural crest origin has been debated, definitive risk factors or mechanisms behind initiation and progression of NB have not been established yet.

Actin and actin-binding proteins play important roles in differentiating neurons.[4] Filamin A (FLNA), an actin-binding protein, is displayed even on the surface of human NB cells and located not only intracellularly.[5] FLNA has been shown to interact with several dopamine receptor proteins using conventional two-hybrid screens.[6] Interestingly, periventricular heterotopia (PH) is a malformation of cortical development characterized by nodules of neurons, ectopically located along the lateral brain ventricles. Mutations occurring in factors regulating vesicle transport impair targeted transport of FLNA to the cell surface within neural progenitors disrupt the attachment and the migration of the neural progenitor cells along the radial glia processes which may contribute to PH formation.[7] Transfection of a dominant-negative construct of ARFGEF2, a vesicle transport ADP-ribosylation factor, in NB cells partially blocked FLNA transport from the Golgi apparatus to the cell membrane, underscoring the importance of this protein in targeted transport of FLNA to the cell surface within neural progenitors.[7] Loss of FLNA impairs neural progenitor proliferation.[8] More interestingly, FLNA is overexpressed in multiple types of human cancer, including NB.[5] Taken together, these findings question whether FLNA is a potentially interesting player as no report exists in the literature regarding the biological importance of FLNA in NB-progression.

In this study, we hypothesized that expression of FLNA would have a role in NB aggressiveness and targeting FLNA in human NB cells would impair tumor progression. To test this hypothesis, we analyzed expression of FLNA in human NB databases and tumors, and silenced expression of *FLNA* mRNA in human NB cells to determine its effect on NB cell function and tumor formation in mice. We also studied the relationship between FLNA expression and NB cell signaling through the STAT3/MYCN pathway.

Materials and Methods

R2 Database

Level of *FLNA* mRNA form both normal prefrontal cortex[9] and mixed DeLattre NB tumor tissues[10] were extracted from this database and analyzed for comparison. According to this database, expression of *FLNA* mRNA was dichotomized into high- and low expression groups based on the median cutoff.[11] Overall survival analysis curves were generated using Kaplan-Meier method with R2 database server (https://hgserver1.amc.nl/cgi-bin/r2/main.cgi). The survival difference between the dichotomized groups was evaluated using log-rank test as previously described.[11] The *P*-value is corrected with Bonferroni's test *P* value.024.

Biobank of Human Neuroblastomas

NB tissues from patients[12] was acquired during surgery and stored at –80°C. Ethical approval was obtained from the Karolinska University Hospital Research Ethics Committee (Approval no. 2009/1369–31/1 and 03–736). Consent for using the tumor samples in scientific research was provided by parents/guardians. In accordance with the approval from the Ethics Committee the informed consent was either written or verbal, and when verbal or written assent was not obtained, the decision was documented in the medical record. Paraffin-embedded and formalin-fixed human NB tumors were sectioned and stained with Hematoxylin & Eosin as described earlier.[13] Images of entire tissue sections stained immunohistochemically using antibodies against FLNA were captured and percentage of positive pixels analyzed by an image analysis program (Biopix software) as described earlier.[13]

Cell Lines, Lentiviral Infections, and Transfections

SKNBE2 (DSMZ, German Collection of Microorganisms and Cell Cultures GmbH), IMR-32, Kelly, and SHSY5 cells (CLS Cell Lines Service GmbH) were cultured and maintained at 37°C with 5% CO_2 and cultured as per manufacturer's instructions. Lentiviral particles encoding control shRNA Ø and shRNA *FLNA* were purchased from Sigma-Aldrich. Stable shRNA cells were generated using the method described previously.[11] Control siRNA Ø and siRNA *FLNA* were purchased from Qiagen and the cells were transfected using Lipofectamine RNAiMAX (ThermoFisher Scientific) according to the manufacturer's instructions. qPCR analysis of mRNA *FLNA* in cultured NB cells was performed as earlier.[14] SH-SY5 cells were transfected using plasmid vector that drives transient overexpression of full-length FLNA as described earlier.[15]

Immunoblotting

Protein lysates from cells were assayed by immunoblotting as described earlier.[11] Primary antibodies directed

against FLNA (Bethyl Laboratories), p-AKT, AKT, p-ERK1/2, ERK1/2, MYCN, p-MEK, p-STAT3, p-NF-κB, p53, cleaved caspase 3 (Cell Signaling), and Actin (Sigma-Aldrich) were used. The densities of triplicate bands were quantified by ImageQuant software (Bio-Rad). Expression levels of FLNA, p53, MYCN and cleaved caspase 3 were normalized to Actin, whereas expression levels of p-AKT and p-ERK1/2, p-STAT3, p-NFκB were normalized to their respective total proteins.

Proliferation Assay

Approximately 1 x 10^4 SKNBE2, IMR32 or SH-SY5 cells were seeded in 96-well plates and transfected with control siRNA Ø and siRNA *FLNA* and allowed to grow for 24 and 48 hours as previously described.[16] Cell numbers were counted using Cell Titer 96 Non-Radioactive Cell Proliferation assay kit from Promega (G4000) as per the manufacturer's instructions.

Migration Assay

For migration assays, 2 x 10^4 SKNBE2 and IMR32 cells were transfected with either control siRNA Ø and siRNA *FLNA* and grown in a modified Boyden chamber (8 µm thick, 8 µm pores in diameter). The number of migrated cells through microporous nitrocellulose filters was counted as described earlier.[17]

Colony Formation Assay

Following transfection of SKNBE2 and IMR32 cells with either control siRNA Ø and siRNA *FLNA* lines, 1 x 10^4 cells were seeded in 12-well plates and allowed to grow into colonies up to 5 days. The media was removed, and colonies were fixed in methanol for 10 min followed by a couple of washes in 1X PBS. Colonies were stained with 1% crystal violet for 10 min and plates were washed carefully with tap water. The plates were dried and images were taken as described earlier.[18]

Spheroid Assay

For spheroid assays, 1 x 10^4 SKNBE2 and IMR32 cells were transfected with either control siRNA Ø or siRNA *FLNA* and suspended in single-cell suspension for hanging drop cultures. Twenty microliters of hanging drop cultures were seeded on a 10 cm plate and allowed to grow up to 7 days. Images were captured from formed spheroids and the total area of spheroid was calculated using Image J software as described earlier.[11]

TUNEL Assay

Approximately 3 x 10^4 SKNBE2 and IMR32 cells transfected with control siRNA Ø or siRNA *FLNA* were grown in chamber slides for 24 hours and assayed for TUNEL assay as per the manufacturer's protocol (Invitrogen). Images were captured and the number of apoptotic cells were manually counted.

Coimmunoprecipitation

Total SKNBE2 cell lysates were first immunoprecipitated with FLNA antibody (Novus Biologicals) and then immunoblotted against STAT3 or FLNA according to the manufacturer's protocol (ThermoFisher Scientific). IgG controls served as intern controls.

Differential Gene Expression Analysis

Total RNA extracted from SKNBE2 cells were transfected with either control siRNA Ø or siRNA *FLNA* and sequenced using the Illumina Sequencing Platform. The read quality was determined using FastQC. The reads were then mapped to the human genome version hg38 (GRCh38) using RNA STAR aligner.[19] Feature counts was used to quantify the reads and differential gene expression was determined using DESeq2. Differentially expressed genes with false discovery rate (FDR) cutoff ≤ 0.01 (Benjamini-Hochberg method) were statistically significant.

Tumor Xenografts

Approximately 4 X 10^6 SKNBE2 cells infected with lentivirus encoding either control shRNA Ø or shRNA FLNA were subcutaneously injected into dorsal back region of five to six-week-old BALB/c nude male mice ($n = 6$ for each group) as described earlier.[17] The tumor area was calculated by measurements of width^2 x length x 0.52 every second day starting a week after. Total proteins from mouse NB tumors were homogenized as described earlier[15] and assayed for immunoblotting for FLNA as above. All the mouse experiments were approved by the Animal Ethical Review Board, University of Gothenburg, Gothenburg, Sweden (Ethical permit number-5.8.18-02708/2017).

Statistical Analysis

GraphPad Prism 6 (GraphPad Software) was used for comparisons between multiple groups with ANOVA, while Student's *t* test was used for comparisons between two groups. All results were reported as the mean ± SEM. A P value < 0.05 was statistically significant.

Results

Increased FLNA Expression is Associated with both Shorter Patient Survival and High-Risk Neuroblastomas

Using R2 Genomics Analysis and Visualization Platform, we observed a significant increase of *FLNA* mRNA in NB tumors ($n = 64$) as compared with normal prefrontal cortex tissues ($n = 44$) ($P < .001$, Figure 1A). Further analysis of *FLNA* expression in the same R2 platform revealed shorter overall survival in NB patients expressing higher levels of *FLNA* mRNA ($n = 21$) compared to patients expressing low *FLNA* levels ($n = 477$; $P < .001$, Figure 1B). Immunohistochemical expression of FLNA was increased

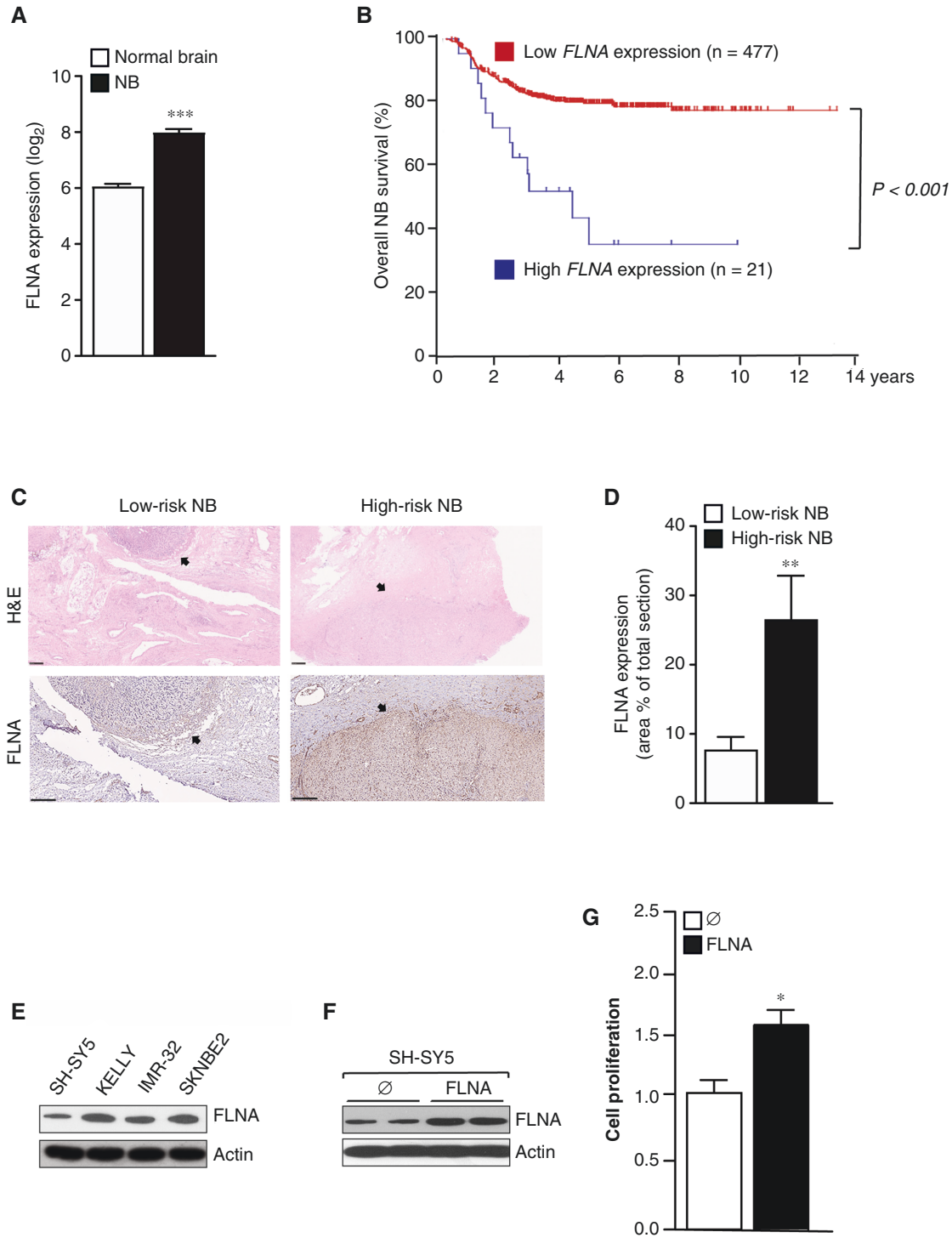

Figure 1. Increased expression of FLNA in NB is associated with shorter patient survival. (A) Expression of *FLNA* mRNA in NB tumor tissues as compared to normal brain tissues. (B) Kaplan-Meier curves for overall survival stratified by mRNA expression of *FLNA* in a cohort of 498 NB patients. Cutoff for high ($n = 477$) or low ($n = 21$) FLNA expression was chosen by Kaplan-Meier analysis. (C) Hematoxylin & Eosin- (upper panels) and FLNA-stained (lower panels) sections of human low-risk ($n = 9$) and high-risk ($n = 9$) NB. Arrows denote neuroblastoma areas. (D) Image analysis of immunohistochemical FLNA expression from entire sections of low- and high-risk human NB. Scale bars represent 100 µm. (E) Multiple NB cell lines expressing FLNA. (F) Expression of FLNA in SH-SY5 cells transfected with a plasmid vector driving FLNA overexpression as compared to empty control vector (Ø). (G) Proliferation assay after transfection of SH-SY5 cells overexpressing of FLNA at 24 hours. Mean ± SEM values of percentage changes in at least triplicate data. * $P < .05$, ** $P < .01$ and *** $P < .001$.

in the entire sections of human high-risk NB compared to low-risk NB (26.71 ± 18.80 *versus* 7.91 ± 6.32%, $P < .01$; Figures 1C,D). Although FLNA expression was also increased in human high-risk NB tumor cells compared to low-risk NB (8.66 ± 15.31% *versus* 1.07 ± 2.93%, $P > .05$), FLNA was mainly expressed by intratumoral vascular endothelial and smooth-muscle cells, as well as connective tissue fibroblasts (Figure 1C). Moreover, FLNA expression varied in multiple cultured NB cell lines (Figure 1E). Relatively low level of FLNA expression in SH-SY5 cells was increased following transfection with a plasmid vector driving transient overexpression of FLNA (Figure 1F). This overexpression resulted in a significant increase in proliferation of SH-SY5 cells by 54% ($P < .05$; Figure 1G).

Expression of FLNA Increases Growth of Neuroblastomas

Transfection of SKNBE2 cells using lentiviral vectors encoding shRNA *FLNA* reduced expression of FLNA by 53% compared with cells infected with control shRNA Ø (Figure 2A). SKNBE2 cells silenced for expression of *FLNA* mRNA formed fewer colonies by 55% ($P < .05$; Figure 2B). We then inoculated these NB cells into mice and observed that SKNBE2 cells silenced for expression of *FLNA* mRNA formed smaller tumors compared to control cells (Figure 2C). Differences in tumor size between these groups were significantly different at day 18 (0.59 ± 0.28 cm^3 *versus* 0.21 ± 0.19 cm^3, $P < .05$) and continued to increase until day 22 (1.98 ± 0.6 cm^3 *versus* 0.66 ± 0.75 cm^3, $P < .01$; Figure 2C). Decreased expression of FLNA by 38% was detected in mouse NB tumors at day 22 (Figure 2D). NB tumors that formed after inoculation of SKNBE2 cells infected with viral vectors encoding either shRNA *FLNA* or control shRNA Ø (Figure 2E upper panels) were immunohistochemically positive for expression of synaptophysin (SYP) (Figure 2E middle panels). The number of proliferating cells in NB that formed after inoculation of SKNBE2 cells silenced for *FLNA* mRNA was reduced by 45% as quantified by immunohistochemical detection of Ki-67 ($P < .05$, Figure 2E lower panels and Figure 2F).

Expression of FLNA Induces Migration and Proliferation of Neuroblastoma Cells

Using transfection of siRNA *FLNA*, we silenced expression of *FLNA* mRNA in SKNBE2 and IMR32 cells. *FLNA* mRNA levels were reduced by 90% in SKNBE2 cells ($P < .05$, Figure 3A) and IMR32 cells by 85% (Supplemental Figure 1A). We assayed these cells for proliferation up to 48 h. In comparison with transfections using control siRNA Ø, we observed that transfection with siRNA *FLNA* reduced proliferation of SKNBE2 cells (1.09 ± 0.39 fold *versus* 0.45 ± 0.02 fold on day 1 and 1.58 ± 0.57 fold *versus* 0.72 ± 0.15 fold on day 2); $P < .05$, Figure 3B) as well as of IMR32 cells (1.01 ± 0.05 fold *versus* 0.51 ± 0.02 fold at day 1 and 1.61 ± 0.21 fold *versus* 0.82 ± 0.11 fold at day 2; $P < .05$, Supplemental Figure 1B). Both SKNBE2 and IMR3 cells transfected with siRNA *FLNA* showed poor migration compared with respective cells transfected with control siRNA Ø (by 41% and 47%, respectively; $P < .05$, Figure 3C and Supplemental Figure 1C) at 16 hours.

FLNA Expression in Neuroblastoma Cells Increases Colony Formation and Spheroid Growth

Following transfection with siRNA *FLNA* at day 5, we observed a reduced number of SKNBE2 cell colonies by 80% ($P < .01$, Figure 3D) and IMR32 cell colonies by 78% ($P < .05$, Supplemental Figure 1D) compared to cells transfected with control siRNA Ø. Compared to respective transfection controls using siRNA Ø, we observed that transfection with siRNA *FLNA* at day 7 reduced the size of spheroids in SKNBE2 (1726 ± 554 μm^2 *versus* 1171 ± 244 μm^2, $P < .01$; Figure 3E) and IMR32 (1176 ± 371 μm^2 *versus* 805 ± 108 μm^2, $P < .01$; Supplemental Figure 1E). Furthermore, we observed that transfection of SKNBE2 cells with siRNA *FLNA* reduced levels of phosphorylated AKT by 60% ($P < .05$, Figure 3F) and phosphorylated ERK1/2 by 72% ($P < .05$, Figure 3G) compared to respective cells transfected with control siRNA Ø. Total AKT or ERK1/2 immunoblots served as internal controls.

Expression of FLNA in Neuroblastoma Cells Protects Against Apoptosis

Following transfection with siRNA *FLNA* at day 1, we observed an increased number of apoptotic SKNBE2 cells from 5% to 34% ($P < .05$, Figure 4A) and IMR32 cells from 4% to 25% of the entire area ($P < .05$, Supplementary Figure 2) compared to respective control cells transfected with siRNA Ø. In SKNBE2 cells, inhibition of *FLNA* mRNA with transfected siRNA *FLNA* reduced phosphorylated levels of NF-κB by 45% ($P < .05$, Figure 4B), but increased levels of both p53 by 155% ($P < .05$, Figure 4C upper blots) and cleaved caspase 3 by 240% ($P < .01$, Figure 4C middle blots) compared to control siRNA Ø.

Expression of FLNA Alters Multiple Cellular Functions of Neuroblastoma Cells

To analyze the transcriptomic profile regulated by FLNA, we knocked down mRNA expression of *FLNA* in human SKNBE2 NB cells using siRNA molecules and performed RNA sequencing. Cluster analysis indicated downregulated expression of 1808 genes and upregulated expression of 2411 genes (Figures 5A) using duplicated sets of control siRNA Ø and triplicated sets of siRNA *FLNA*. Both *STAT3* and *MYCN* were among genes showing downregulation following knockdown of *FLNA*. Furthermore, gene ontology analysis of the differentially expressed genes showed that majority of the upregulated genes were associated with regulation of apoptosis or autophagy (Figure 5B), whereas downregulated genes played a role in pathways involved in angiogenesis, development, cytoskeleton, or cellular migration (Figure 5C).

FLNA Interacts with STAT3

Total SKNBE2 cell lysates were immunoprecipitated with antibodies against FLNA and then immunoblotted with

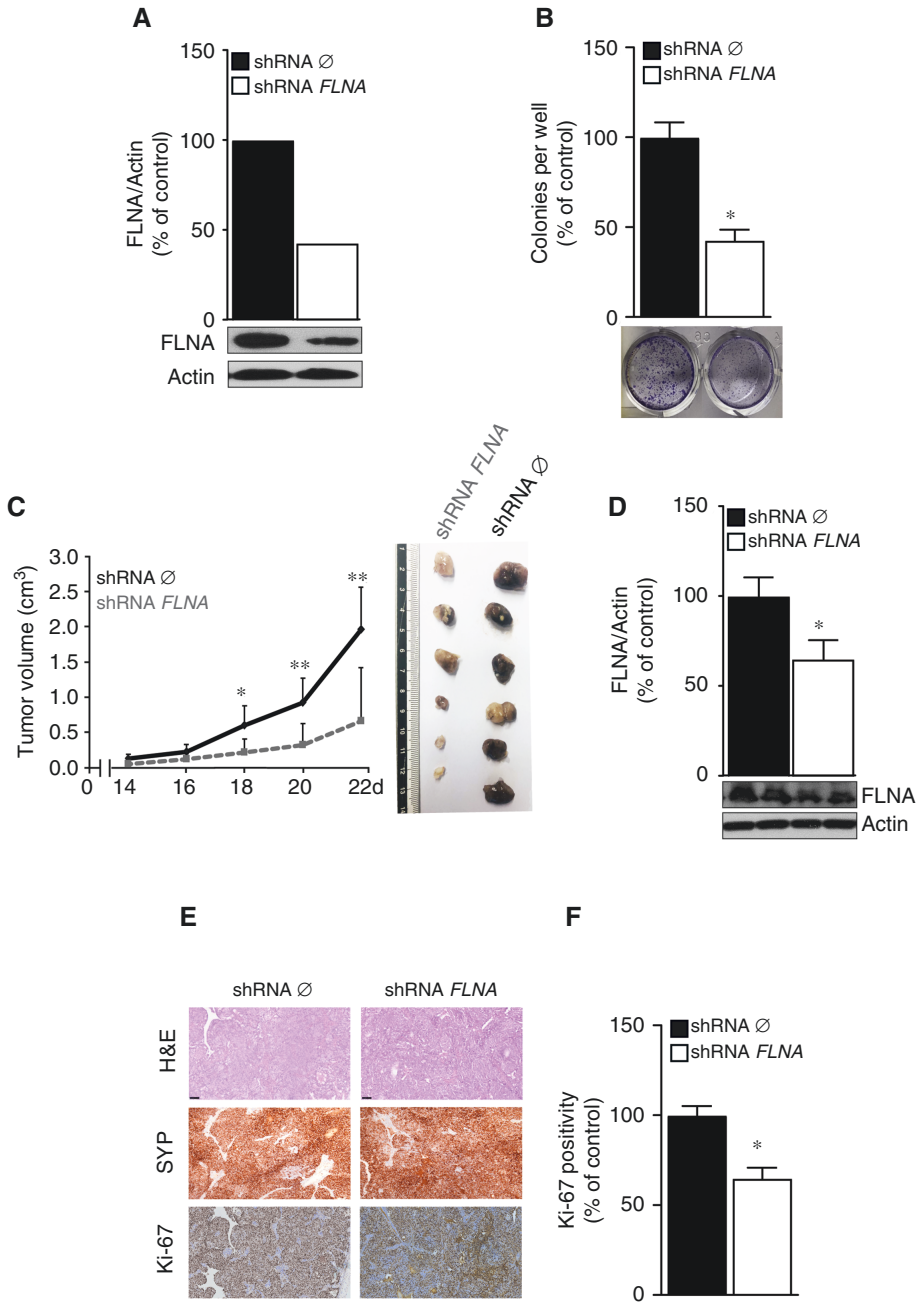

Figure 2. Expression of FLNA increases NB growth. Immunoblot analysis of FLNA (A) and number of colonies up to 5 days (B) in SKNBE2 cells infected with either lentiviral vector expressing shRNA Ø or shRNA *FLNA*. (C) Size of NB formed following inoculation of SKNBE2 cells infected with either lentiviral vector expressing shRNA Ø or shRNA *FLNA* in BALB/c nude mice up to 22 days (left panels) and representative images of NB tumors (right panels). (D) Quantification of immunoblot analysis of FLNA in mouse NB formed after inoculation of SKNBE2 cells either expressing or lacking FLNA. (E) Representative images of Hematoxylin & Eosin-stains (upper panels), immunohistochemical detection of synaptophysin (SYN; middle panels) and Ki67 (lower panels) of shRNA Ø and shRNA FLNA tumors (upper panels) in NB formed by SKNBE2 cells infected with lentiviral vector expressing either shRNA Ø or shRNA FLNA. Scale bars represent 100 μm. (F) Quantification of immunohistochemical detection of Ki67. Mean ± SEM values of percentage changes in at least triplicate data. * $P < .05$ and ** $P < .01$.

anti-STAT3 antibody. STAT3 was identified as an interaction partner of FLNA (Figure 6A). Transfection of these cells with siRNA *FLNA* reduced expression of FLNA by 60% ($P < .01$, Figure 6B). Following transfection with siRNA *FLNA*, we observed reduced levels of phosphorylated p-STAT3^{727} by 48% ($P < .05$, Figure 6C left panel) and p-STAT3^{705} by 45% ($P < .05$, Figure 6C right panel). Furthermore, transfection of these cells with siRNA *FLNA*

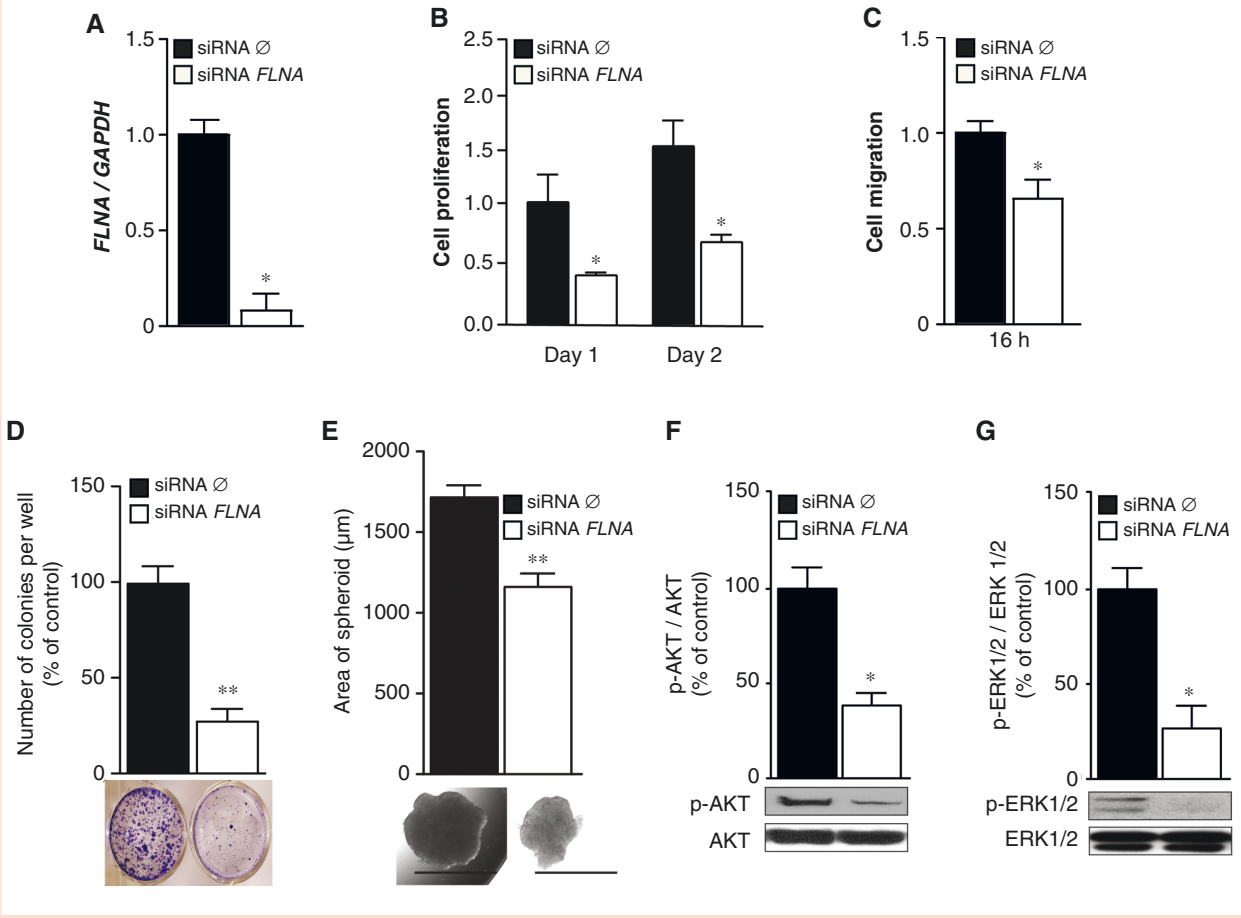

Figure 3. Expression of FLNA induces migration, proliferation, colony formation, and spheroid growth of NB cells. qPCR analysis of mRNA *FLNA* (A), number of cells at 24 hours and 48 hours (B), and number of migrated cells assayed in modified Boyden's chamber up to 16 hours in SKNBE2 cells transfected with either siRNA Ø or siRNA *FLNA*. The number of colonies up to 5 days (D) and spheroid areas up to 7 days (E). Scale bars represent 100 µm. Immunoblots of p-AKT (F) and p-ERK1/2 (G) in SKNBE2 cells transfected with either siRNA Ø or siRNA *FLNA*. *GAPDH* served as internal loading control for qPCR, whereas total AKT or ERK1/2 proteins served as internal loading control for immunoblots. Mean ± SEM values of percentage changes in at least triplicate data. * $P < .05$ and ** $P < .01$.

resulted in reduced expression of *MYCN* mRNA by 72% ($P < .05$, Figure 6D left panel) as well as MYCN protein by 51% ($P < .05$, Figure 6D right panel).

Discussion

NB represents the most common extracranial solid tumor and the fourth most common malignant tumor in childhood. Children with high-risk NB often have poor outcomes with low survival rates, despite several treatment options. At present, no specific molecular targets or chemotherapeutic vulnerabilities have been identified, which limits the development of therapeutic strategies for NB. Therefore, novel therapeutic options are thus urgently needed. To the best of our knowledge, the present study is the first to investigate the novel function of FLNA in NB development. Here, increased expression of FLNA was detected in patients with shorter survival rates and high-risk NB tumors. These associations provided the basis for further study of the mechanism of action for FLNA in multiple NB cell lines. Secondly, the present study first observed that the lack of FLNA leads to impaired proliferation, migration, and colony formation, as well as increased apoptosis of NB cells *in vitro* and NB cells lacking FLNA form smaller tumors *in vivo*. Thirdly, the present study identified a novel function of FLNA regulating expression of MYCN by binding to STAT3.

Our initial data on an association between elevated FLNA expression and more unfavorable patient survival as well as high-risk NB tumors is exciting. To study the biological function of increased FLNA expression in NB cells, we conducted both cell culture assays and bioinformatics analysis. The results showed that lack of FLNA downregulates expression of multiple groups of cellular migratory genes, which was consistent with our *in vitro* experiments. We observed that in the absence of FLNA, human NB cells migrate, proliferate, and form colonies less as well as smaller spheroids, which are partly explained by the reduced levels of phosphorylated AKT and ERK1/2. The PI3K/AKT and ERK/MAPK pathways are both

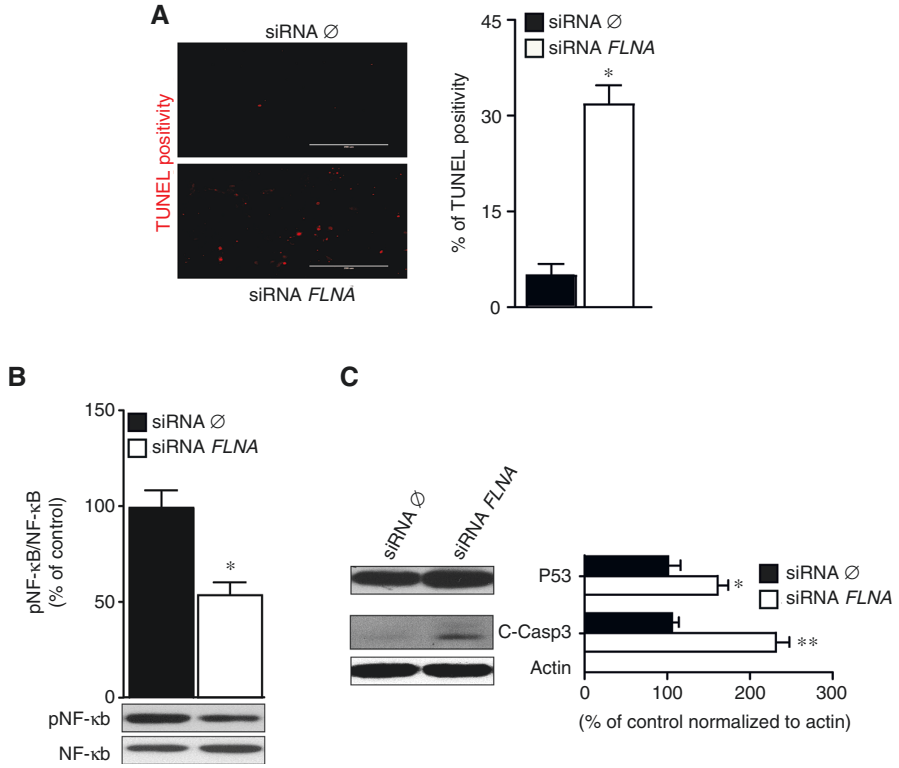

Figure 4. Expression of FLNA in human NB cells protects against apoptosis. (A) TUNEL staining and number of apoptotic SKNBE2 cells transfected with either siRNA Ø or siRNA *FLNA*. Scale bars represent 200 μm. (B) Representative immunoblots and quantification of band intensities of pNF-κB. (C) Representative immunoblots and quantification of band intensities of p53 and cleaved caspase 3 in SKNBE2 cells transfected with either siRNA Ø or siRNA *FLNA*. Total NF-κB and actin served as internal loading control. Mean ± SEM values for percentage changes in at least triplicate data. * $P < .05$ and ** $P < .01$.

abnormally activated in many cancer types, including NB.[20] Recently, it has been proposed that selecting pan-AKT inhibitors rather than isoform-specific drugs to synergize with first-line chemotherapy treatment should be considered for clinical trials for aggressive MYCN-driven NB.[21] Similarly, small molecule inhibitors effectively suppress NB tumor growth in experimental models via inhibiting ERK/MAPK signaling.[22,23]

Dysregulation of apoptotic pathways has an important role in cancer development due to mutations or DNA amplification in oncogenes such as MYC. A mediatory role of FLNA in anti-NB IgM-induced apoptosis has been proposed.[5] In this study, we detected increased expression of apoptotic p53 and cleaved caspase 3 and reduced MYCN expression, as well as multiple gene groups involved in apoptosis and autophagy in NB cells lacking FLNA. These results point to FLNA as an anti-apoptotic role in NB. High-risk NBs often harbor structural chromosomal alterations, including amplified *MYCN* and MYCN-mediated over-activation of the metaphase-anaphase checkpoint synergizes with loss of p53 function to prevent arrest or apoptosis of NB cells.[24] Besides, MYCN-directed centrosome amplification requires MDM2-mediated suppression of p53 activity in NB cells.[25] Cytoskeletal arrangement is independent of caspase activation[26] and cytoskeletal disruption triggers apoptosis in NB cells.[27] Furthermore, binding of FLNA to actin filaments is regulated by calcium and calmodulin[28] and calcium/calmodulin-dependent protein kinase-related peptides induce neuronal apoptosis.[29]

STAT3 is an oncogenic transcription factor that has been implicated in many human cancers, including NB.[30] Several oncogenic targets of STAT3 have recently been identified including MYC[31] and inhibition of STAT3 with antisense oligonucleotides decreases NB tumorigenicity and increases chemosensitivity.[32] Interestingly, inhibition of STAT3 with an orally active JAK inhibitor decreases tumor growth in NB both *in vitro* and *in vivo*.[33] Furthermore, the MYCN oncogene has been proposed as a specific and selective drug target for NB.[34] Regulation of MYCN expression is not completely known. However, downregulation of MYCN leads to decreased proliferation and differentiation, emphasizing the importance of MYCN signaling in NB.[35] In this study, we identified STAT3 as an interacting partner of FLNA and then showed that both expression of phosphorylated STAT3 and MYCN was reduced in NB cells lacking FLNA. Similar to STAT3, FLNA interacts with other transcriptional factors such as HIF-1α[15] and SMAD2[13] to regulate expression of VEGF or c-MET, respectively. For transcriptional regulation of these target genes, cleavage of FLNA by calpains as well as nuclear transportation of these transcriptional factors by cleaved C-terminal

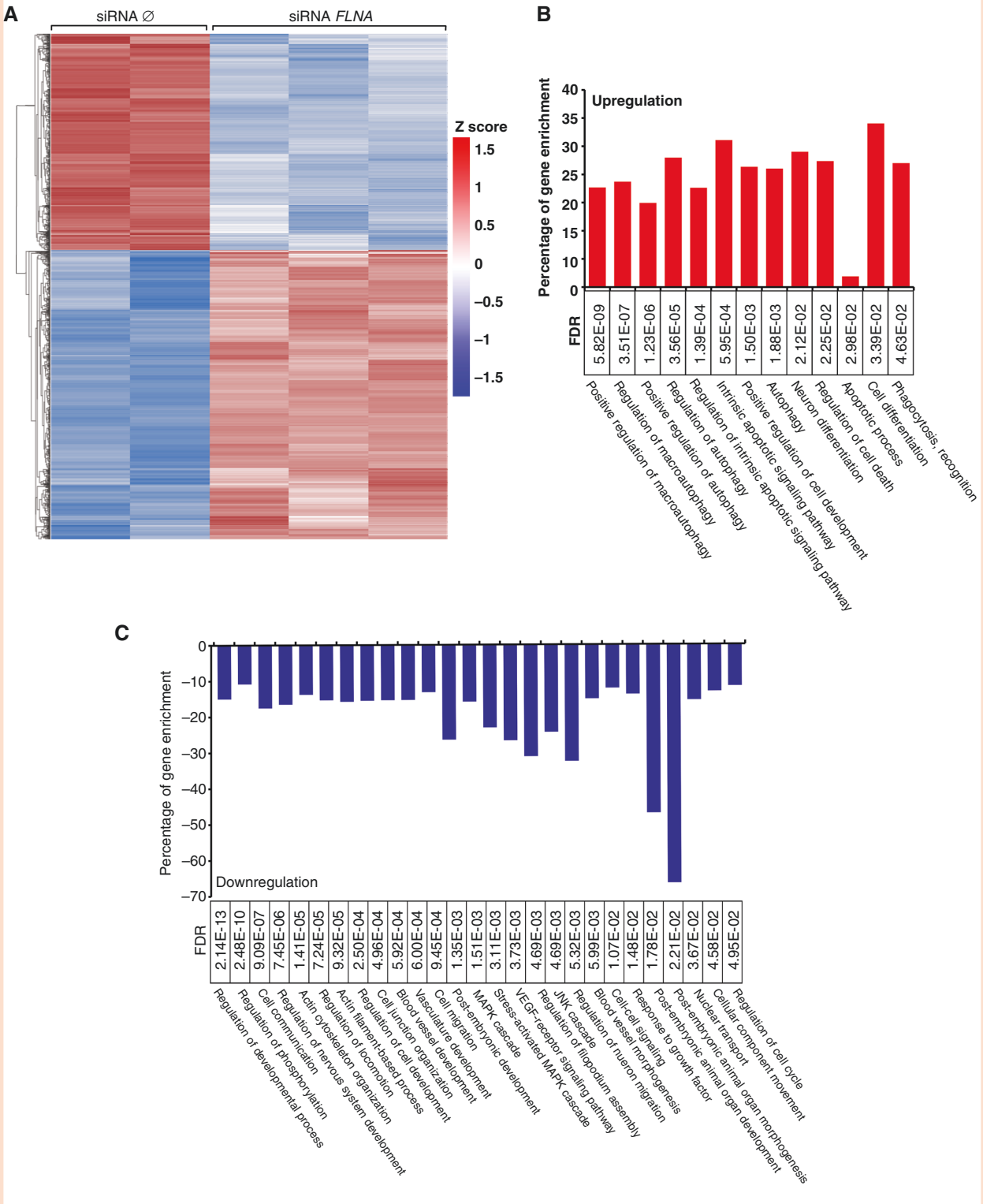

Figure 5. Expression of genes that are differentially expressed by the absence FLNA in multiple replicates of human SKNBE2 NB cells. (A) Cluster analysis of gene expression following knockdown of mRNA *FLNA*. Significantly upregulated genes (red, B) or downregulated genes (blue, C) grouped according to their biological functions using gene ontology analysis. Fold changes ranging from 1.5 to –1.5 colored according to Z scores. Altered gene expressions grouped into their different function and presented as percentage of gene enrichment. Level of significant changes presented as false discovery rates (FDR) in boxes.

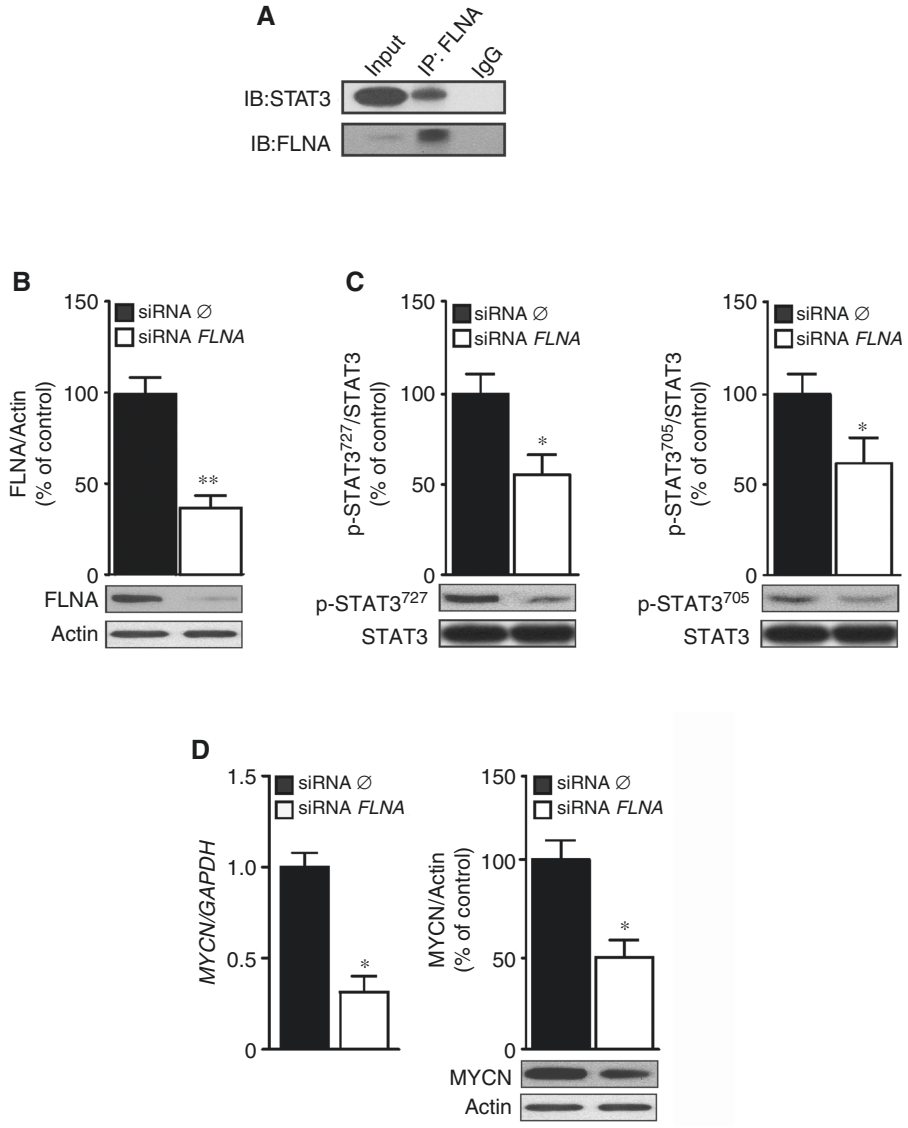

Figure 6. FLNA interacts with STAT3 and alters expression of MYCN. (A) For the coimmunoprecipitation assay, SKNBE2 NB cells were lysed for protein extraction, immunoprecipitated with FLNA and then immunoblotted with STAT3 antibodies. IgG served as negative controls. Representative immunoblots and quantitative analysis of band intensities of FLNA (B) and, p-STAT3^{727} and p-STAT3^{705} (C) in SKNBE2 NB cells transfected with either siRNA Ø or siRNA *FLNA*. Actin and total STAT3 served as internal loading control. (D) qPCR analysis of *MYCN* mRNA (left panels) as well as representative immunoblots and quantification of MYCN band intensities in SKNBE2 NB cells transfected with either siRNA Ø or siRNA *FLNA*. Mean ± SEM values of fold or percentage changes in at least triplicate data. * $P < .05$ and ** $P < .01$.

fragment of FLNA have been discussed. Whether there is a similar FLNA biology that contributes MYCN activity as a result of FLNA interaction with STAT3 in NB needs to be further explored.

These data enhance our understanding of how cytoskeletal FLNA mediates aggressive behavior of NB. The finding of increased FLNA expression in shortened survival and high-risk NB points to FLNA as a potential prognostic biomarker in NB etiology. Overall, we have established a causative correlation between FLNA-dependent expression in NB cell function *in vitro* and NB tumor development *in vivo*, identifying FLNA as a potential target to reduce NB growth.

Supplementary material

Supplemental material is available at *Neuro-Oncology Advances* online.

Keywords

filamin | high-risk | MYCN | neuroblastoma | STAT3

Funding

This work was supported by the Strategic Fund from the Institute of Biomedicine, University of Gothenburg, the Swedish Cancer Foundation (CAN2017-0171 and CAN2018/591), the Agreement between Swedish central government and Region Västra Götaland on physician education and clinical research (ALF) fund ((ALFGBG-495961 and ALFGBG-965280) from the Sahlgrenska Academy Hospital in the Region Västra Göteland, the Assar Gabrielsson's Foundation (FB20-87) and the Adlerbertska Research Foundation (GU 2020/751).

Conflict of interest statement. The authors disclose no potential conflicts of interest.

Authorship statement. Concept and design: S.B., L.M.A. Provision of cell lines, study material, patient data: P.K.J., B.P., P.K., J.I.J., C.K. Experiment execution and data interpretation: S.B., P.K.J., B.P., S.D., C.K., L.M.A. Manuscript writing: S.B., L.M.A. Final approval of manuscript: All authors.

References

1. Brodeur GM. Neuroblastoma: biological insights into a clinical enigma. *Nat Rev Cancer.* 2003;3(3):203–216.
2. Shimada H, Ambros IM, Dehner LP, et al. Terminology and morphologic criteria of neuroblastic tumors: recommendations by the International Neuroblastoma Pathology Committee. *Cancer* 1999;86(2):349–363.
3. Park JR, Bagatell R, London WB, et al. Children's Oncology Group's 2013 blueprint for research: neuroblastoma. *Pediatr Blood Cancer.* 2013;60(6):985–993.
4. Abd-el-Basset EM, Ahmed I, Fedoroff S. Actin and actin-binding proteins in differentiating astroglia in tissue culture. *J Neurosci Res.* 1991;30(1):1–17.
5. Bachmann AS, Howard JP, Vogel CW. Actin-binding protein filamin A is displayed on the surface of human neuroblastoma cells. *Cancer Sci.* 2006;97(12):1359–1365.
6. Li M, Bermak JC, Wang ZW, Zhou QY. Modulation of dopamine D(2) receptor signaling by actin-binding protein (ABP-280). *Mol Pharmacol.* 2000;57(3):446–452.
7. Lu J, Tiao G, Folkerth R, et al. Overlapping expression of ARFGEF2 and Filamin A in the neuroependymal lining of the lateral ventricles: insights into the cause of periventricular heterotopia. *J Comp Neurol.* 2006;494(3):476–484.
8. Lian G, Lu J, Hu J, et al. Filamin a regulates neural progenitor proliferation and cortical size through Wee1-dependent Cdk1 phosphorylation. *J Neurosci.* 2012;32(22):7672–7684.
9. Breen MS, Ozcan S, Ramsey JM, et al. Temporal proteomic profiling of postnatal human cortical development. *Transl Psychiatry.* 2018;8(1):267.
10. Janoueix-Lerosey I, Lequin D, Brugieres L, et al. Somatic and germline activating mutations of the ALK kinase receptor in neuroblastoma. *Nature* 2008;455(7215):967–970.
11. Mondal T, Juvvuna PK, Kirkeby A, et al. Sense-antisense lncRNA pair encoded by locus 6p22.3 determines neuroblastoma susceptibility via the USP36-CHD7-SOX9 regulatory axis. *Cancer Cell* 2018;33(3):417–434.e7.
12. Mitra S, Muralidharan SV, Di Marco M, et al. Subcellular distribution of p53 by the p53-responsive lncRNA NBAT1 determines chemotherapeutic response in neuroblastoma. *Cancer Res.* 2021;81(6):1457–1471.
13. Zhou AX, Toylu A, Nallapalli RK, et al. Filamin a mediates HGF/c-MET signaling in tumor cell migration. *Int J Cancer.* 2011;128(4):839–846.
14. Bandaru S, Ala C, Salimi R, et al. Targeting filamin A reduces macrophage activity and atherosclerosis. *Circulation* 2019;140(1):67–79.
15. Zheng X, Zhou AX, Rouhi P, et al. Hypoxia-induced and calpain-dependent cleavage of filamin A regulates the hypoxic response. *Proc Natl Acad Sci USA.* 2014;111(7):2560–2565.
16. Pandey GK, Mitra S, Subhash S, et al. The risk-associated long noncoding RNA NBAT-1 controls neuroblastoma progression by regulating cell proliferation and neuronal differentiation. *Cancer Cell* 2014;26(5):722–737.
17. Bandaru S, Zhou AX, Rouhi P, et al. Targeting filamin B induces tumor growth and metastasis via enhanced activity of matrix metalloproteinase-9 and secretion of VEGF-A. *Oncogenesis* 2014;3:e119.
18. Salimi R, Bandaru S, Devarakonda S, et al. Blocking the cleavage of filamin A by calpain inhibitor decreases tumor cell growth. *Anticancer Res.* 2018;38(4):2079–2085.
19. Dobin A, Davis CA, Schlesinger F, et al. STAR: ultrafast universal RNA-seq aligner. *Bioinformatics* 2013;29(1):15–21.
20. Zafar A, Wang W, Liu G, et al. Molecular targeting therapies for neuroblastoma: progress and challenges. *Med Res Rev.* 2021;41(2):961–1021.
21. Le Grand M, Kimpton K, Gana CC, et al. Targeting functional activity of AKT has efficacy against aggressive neuroblastoma. *ACS Pharmacol Transl Sci* 2020;3(1):148–160.
22. Li H, Yu Y, Zhao Y, et al. Small molecule inhibitor agerafenib effectively suppresses neuroblastoma tumor growth in mouse models via inhibiting ERK MAPK signaling. *Cancer Lett.* 2019;457:129–141.
23. Subramonian D, Phanhthilath N, Rinehardt H, et al. Regorafenib is effective against neuroblastoma in vitro and in vivo and inhibits the RAS/MAPK, PI3K/Akt/mTOR and Fos/Jun pathways. *Br J Cancer.* 2020;123(4):568–579.
24. Gogolin S, Batra R, Harder N, et al. MYCN-mediated overexpression of mitotic spindle regulatory genes and loss of p53-p21 function jointly support the survival of tetraploid neuroblastoma cells. *Cancer Lett.* 2013;331(1):35–45.
25. Slack AD, Chen Z, Ludwig AD, Hicks J, Shohet JM. MYCN-directed centrosome amplification requires MDM2-mediated suppression of p53 activity in neuroblastoma cells. *Cancer Res.* 2007;67(6):2448–2455.
26. Vilarino N, Nicolaou KC, Frederick MO, Vieytes MR, Botana LM. Irreversible cytoskeletal disarrangement is independent of caspase activation during in vitro azaspiracid toxicity in human neuroblastoma cells. *Biochem Pharmacol.* 2007;74(2):327–335.
27. Cabado AG, Leira F, Vieytes MR, Vieites JM, Botana LM. Cytoskeletal disruption is the key factor that triggers apoptosis in okadaic acid-treated neuroblastoma cells. *Arch Toxicol.* 2004;78(2):74–85.
28. Nakamura F, Hartwig JH, Stossel TP, Szymanski PT. Ca2+ and calmodulin regulate the binding of filamin A to actin filaments. *J Biol Chem.* 2005;280(37):32426–32433.
29. Schenk GJ, Engels B, Zhang YP, et al. A potential role for calcium/calmodulin-dependent protein kinase-related peptide in neuronal apoptosis: in vivo and in vitro evidence. *Eur J Neurosci.* 2007;26(12):3411–3420.
30. Carpenter RL, Lo HW. STAT3 target genes relevant to human cancers. *Cancers* 2014;6(2):897–925.
31. Barre B, Vigneron A, Coqueret O. The STAT3 transcription factor is a target for the Myc and riboblastoma proteins on the Cdc25A promoter. *J Biol Chem.* 2005;280(16):15673–15681.

32. Odate S, Veschi V, Yan S, et al. Inhibition of STAT3 with the generation 2.5 antisense oligonucleotide, AZD9150, decreases neuroblastoma tumorigenicity and increases chemosensitivity. *Clin Cancer Res.* 2017;23(7):1771–1784.
33. Yan S, Li Z, Thiele CJ. Inhibition of STAT3 with orally active JAK inhibitor, AZD1480, decreases tumor growth in neuroblastoma and pediatric sarcomas *in vitro* and *in vivo*. *Oncotarget* 2013;4(3):433–445.
34. Pession A, Tonelli R. The MYCN oncogene as a specific and selective drug target for peripheral and central nervous system tumors. *Curr Cancer Drug Targets.* 2005;5(4):273–283.
35. Westermark UK, Wilhelm M, Frenzel A, Henriksson MA. The MYCN oncogene and differentiation in neuroblastoma. *Semin Cancer Biol.* 2011;21(4):256–266.